

*Запропонований спосіб обробки зовнішньої та внутрішньої конічних поверхонь цапфи і вставки, що являють собою пару тертя ковзання опори розчинозмішувача. Обробка полягає у тому, що на конічні поверхні деталей, які були попередньо підготовлені точінням, наноситься зносостійкий матеріал у вигляді твердосплавного порошку на основі нікелю. Нанесення відбувається спеціальним пальником із бункером-дозатором, у який засипається порошок. Внаслідок змішування горючого газу (ацетилен та кисень) у пальникові із порошком з бункера, відбувається розплавлення.*

*Під час реалізації даного технологічного процесу із застосуванням методів математичного моделювання було знайдено оптимальні режимні параметри (витрата порошку ПГ10Н-01 – 33,5 г/хв.; витрата кисню – 7,0 л/хв.; тиск ацетилену – 0,043 МПа) газополуменевого наплавлення, які забезпечили максимальний ефект, тобто найбільшу міцність зчеплення (45 МПа) наплавленого покриття. Випробування якості наплавленого покриття здійснювалось за допомогою штифтового методу визначення міцності зчеплення нового покриття із основою на розривній машині.*

*Серія експериментальних досліджень щодо підвищення абразивної стійкості опори ковзання, а саме порівняння наплавленого покриття із іншими загальновідомими зносостійкими матеріалами, такими як сталь ШХ15, ХВГ, здійснювалась на спеціально розробленому дослідному стенді. Його конструкцію розроблено на базі вертикально-свердлильного настільного верстата із адаптацією його до умов робочого процесу, що відбувається у корпусі розчинозмішувача. Це наявність абразивного середовища, радіальних і осьових зусиль. Для визначення осьового навантаження на опору запропоновано конструкцію гідравлічного пристосування, яке складається із манометра, поршня, гільзи та кульки. Осьове навантаження знайдено для найбільш несприятливих умовах роботи змішувача. Його значення було реалізовано на дослідному стенді зношування. Окрім цього, проведено серію експериментальних досліджень із визначення оптимального кута конуса при вершині цапфи і вставки конічної опори ковзання для мінімального зношування.*

*Використання запропонованого способу газополуменевого наплавлення дозволить суттєво підвищити абразивну та корозійну стійкість опори ковзання, подовживши термін експлуатації розчинозмішувача у цілому, розширити міжремонтний цикл обладнання для приготування будівельних розчинних сумішей*

*Ключові слова: газополуменеве наплавлення, абразивне зношування, опора ковзання, твердосплавний порошок, технологічний процес*

UDC 667.637.22:620.178.16

DOI: 10.15587/1729-4061.2020.193510

## IMPROVING THE ABRASIVE RESISTANCE OF A SLIDE FRAME IN A MORTAR MIXER

S. Popov

PhD, Associate Professor\*

E-mail: psv26@i.ua

S. Gnitko

PhD, Associate Professor\*

E-mail: novtehwest@gmail.com

A. Vasyliiev

PhD, Associate Professor\*

E-mail: 7331@i.ua

\*Department of Construction

Machinery and Equipment

National University

«Yuri Kondratyuk

Poltava Polytechnic»

Pershotravnevyi ave., 24,

Poltava, Ukraine, 36011

Received date 09.01.2020

Accepted date 23.01.2020

Published date 24.02.2020

Copyright © 2020, S. Popov, S. Gnitko, A. Vasyliiev

This is an open access article under the CC BY license

(http://creativecommons.org/licenses/by/4.0)

### 1. Introduction

The operation of technological machines is accompanied by phenomena and processes that could result in their failure. Among them, abrasive wear is worth noting. This is the surface destruction of machine parts as a result of their interaction with high hardness particles at high speed of interaction. These particles include: rigidly fixed grains, loose particles, the particles that move freely inside the gaps of conjugated parts, as well as the loose particles sucked to a jet by a liquid or gas [1].

There are many technological methods to improve the abrasive resistance of machine parts exposed to friction, namely, forming a galvanic coating, anodizing, saturation, surfacing (manual, arc, by covered electrodes; under a flux, by wires and strips; in the environment of protective gases, by electrodes, self-protective powdered wires; electroslog, plasma, laser, elec-

tron beam, induction, gas-flame), chill casting, plasma tempering, laser hardening. Each method has its own scope of application, the advantages and disadvantages. Based on the detailed analysis [2, 3], in order to improve the abrasive resistance of the conical slide frame in the working body of a mortar mixer, operated in a soluble mixture used for construction, a method of gas-flame surfacing was recommended. That makes it possible to flexibility and independently control a working temperature, control the consumption of a surfaced material; it does not require any complex technological equipment, nor significant energy costs. In addition, it ensures the possibility to adjust the thickness of a surfaced layer through different inclination angles of a workpiece; and it is characterized by a low cost.

Therefore, it is a relevant task to investigate the processes that are associated with the increased resistance to abrasive wear due to using the technology for gas-flame surfacing a wear-

resistant material on the parts of a friction pair in a slide frame. The frame operates as a part of the working body (belt auger) of a mortar mixer for preparing soluble mixtures used for construction.

**2. Literature review and problem statement**

The slide frame, shown in Fig. 1, represents a completely assembled unit included in the mobile mortar mixer equipped with a pump [4].

The principle of frame operation is described in detail in [2]. A pair of friction in the frame is formed through the interaction between insert 5 (Fig. 2) and wrist pin 12 (Fig. 3). The frame is adjustable. Its special feature is that it completely replaces a standard one (a roll frame), which was located from the outside of the mixer body and whose tightness deteriorated over time.

In [3], authors noted that the long-term industrial tests of a frame are accompanied by significant wear of the insert and wrist pin. The working body of the mixer rubs against its casing's bottom. This leads to a gradual failure of the working shaft in a screw mixer, due to its sagging and ultimate jamming.

Paper [5] was an attempt to investigate the friction of a frame's working surfaces under the action of the applied load. The wear magnitude in the wrist pin and insert was calculated. It was established that the pressure at the surface of the wrist pin and insert obeys a hyperbolic dependence. It was proposed to use wear-resistant materials at the rubbing surfaces. However, no experimental research was conducted.

In [6], authors report that machines and mechanisms operate under different conditions, which is why their wear is affected by the working environment in which the friction and wear occur.

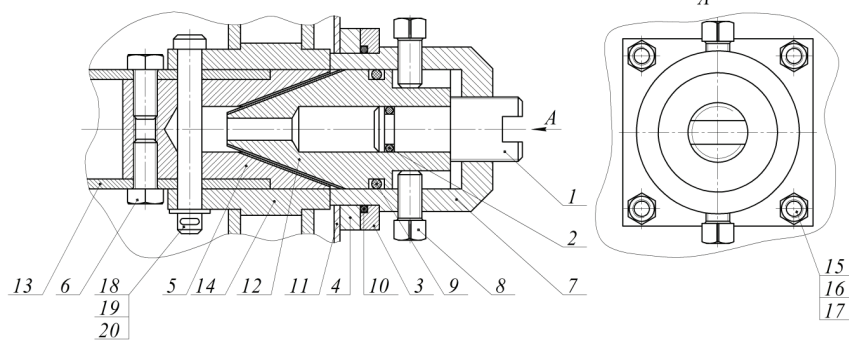


Fig. 1. A slide frame: 1 – pressing screw; 2, 9, 10 – sealing rings; 3, 4 – flange; 5 – insert; 6 – screw; 7 – body; 8 – adjustment screw; 11 – mixer wall; 12 – wrist pin; 13 – mixer shaft; 14 – pinwheel; 15 – pintle; 16 – nut; 17 – shim; 18 – finger; 19 – cotter pin; 20 – pin

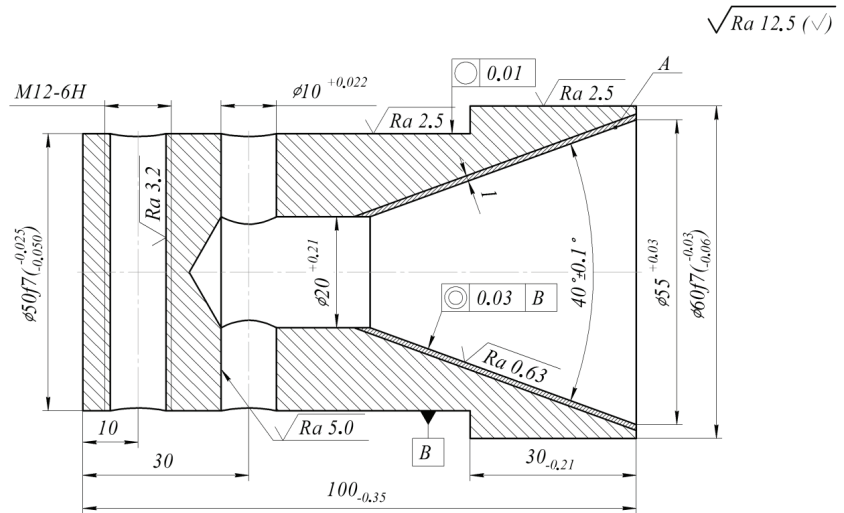


Fig. 2. The insert in a slide frame

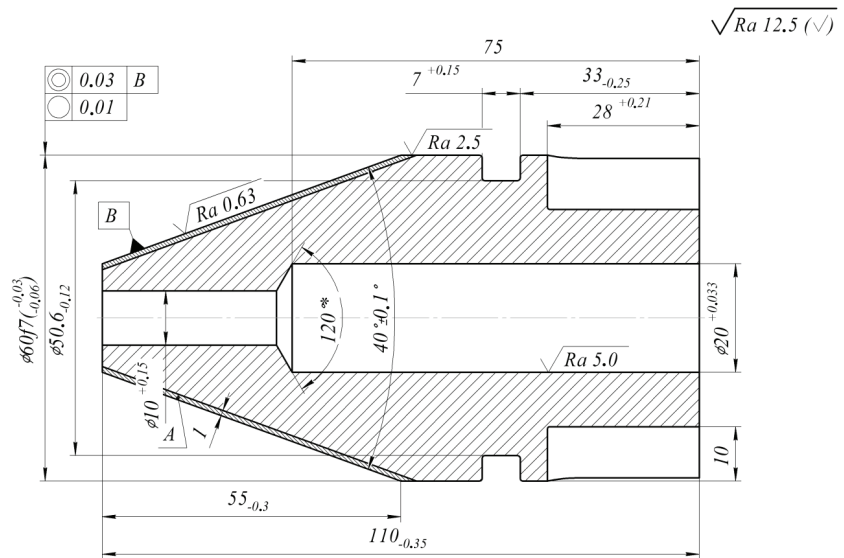


Fig. 3. The wrist pin in a slide frame

The reported study proved that the abrasive resistance of steels depends on their hardness, chemical composition, and the structure of a surface layer. For the non-alloyed steels with a stable structure, wear resistance is directly proportional to the hardness of a friction surface. The alloying elements, for example, chromium, improve durability. It was proposed to enhance the durability of steels by ionic nitriding. The use of gas-flame surfacing was not given due attention.

Work [7] applied the methods of mathematical modeling to examine the process of gas-flame surfacing involving a nickel-based powder. The model was used to assess a time-dependent change in the volume of a coating's metal, since the dissolution of carbide originates from the particles shaped in spheres and cylinders. In addition, the authors investigated the motion speed and temperature of the powder

particles, depending on their shape and size, as well as the initial parameters of the technological process.

The same researchers mathematically modeled the factors of a surfaced coating in the system WC-Ni. These include a temperature change, a hardening rate, and the thermal interactions between a coating's layers [8]. The conditions for forming the proper structures within a coating and a substrate were defined. The study noted that the main issue worth investigating was to search for the optimum technological parameters of the surfacing process, which would ensure the maximum performance of the coating.

Work [9] reported a study into the erosion-corrosion characteristics of self-fluxing coatings in the system Ni-Cr-Mo-Si-B, applied on the carbon (BS970 EN8) and stainless (UNS S31603) steels. The authors compared the samples of conventional surfacing to those obtained under conditions of vacuum with the saturation by a polymeric material. The working environment during the research was a jet of seawater. The disadvantage of the examined coatings was that the polymer did not change the erosion-corrosion performance of the newly formed surface, although a slight increase in resistance was observed anyway. Therefore, the issue of protecting metallic articles against erosion and corrosion destruction in seawater has remained open.

A detailed study into the microstructure of a surfaced coating (a nickel-chromium base) with a thickness of 200  $\mu\text{m}$  was reported in [10]. X-ray diffraction and electron microscopy were applied. The coatings had a layered structure as a result of deposition and cooling of the sequentially and partially melted splashes. The structure of matrices, enriched with nickel and chromium, was investigated. The durability of newly formed surfaces was left unaddressed. The authors only stated that the microhardness of a newly formed coating containing boron and carbon was 6 GPa.

In [11], authors proposed the application of a hard alloyed nickel-based wear-resistant powder on working surfaces using surfacing. Conventional carbon and stainless steels were used for comparison. The coating resistance against erosion was investigated by using a cavitation apparatus. A given study addressed not the abrasive resistance of a coating, but the cavitation one.

The properties of a wear-resistant layer based on nickel were investigated in [12]. A special feature is that this layer was additionally reinforced with the titanium carbide and boron carbide particles. The samples demonstrated excellent wear-resistant properties; however, the impact viscosity decreased. That could subsequently lead to the formation of cracks. The latter would pass throughout the entire surfaced layer, which is not acceptable.

Improving the resistance against a high-temperature abrasion by the  $\text{Cr}_3\text{C}_2$ -NiCr coatings with the addition of WC, which were applied by high-speed surfacing followed by a thermal treatment, was described in work [13]. To identify the effect exerted by adding tungsten carbide on the hardness and abrasion resistance of the newly formed surfaces, the authors investigated powders obtained in various ways. The applied coatings were exposed to the thermal treatment to simulate operating conditions at elevated temperatures. The microstructure was studied by an X-ray diffraction method; the hardness of the coatings – by micro- and nano-indenters, over a temperature range from ambient to 800 °C. The coating hardness did improve after thermal processing. That was predetermined by the release of secondary carbides and by strengthening the solid adhesion solution by tungsten.

In addition, the study proved that the experimental coatings had high durability at room and elevated temperatures. The disadvantage is the difficulty of obtaining these powders, as well as the need for the further thermal treatment. This makes the technology more expensive and requires additional equipment.

Work [14] studied the application of nickel and nickel-inconel powders on the surfaces of stainless steels. The microstructure of coatings was examined using the methods of X-ray diffraction, electron microscopy, energy dispersive X-ray spectroscopy, and by testing for hardness. The cavitation study tested resistance against erosion. Adding inconel increases the hardness and resistance of coatings. However, cavitation erosion reduces the magnitude of fatigue strength in the obtained coatings.

The results from our analysis of the scientific literature have revealed a large body of research into the surfacing process involving the wear-resistant nickel-based powders. The method has become quite common given its relative simplicity and low cost. Along with this, there remain the problematic issues related to determining the optimal technological parameters of surfacing for specific cases and the microstructure of newly formed coatings, their effect on abrasive and corrosion properties of articles, the strength of adhesion to a main material, cooling rate and the hardening of the applied material, the processes of interaction between the newly formed layers, etc. In addition, of interest is the processes of combustion of various combustible gases and vapors in a mixture with oxygen, the uniform supply of a surfaced material to the high-temperature combustion zone. The application of the nickel-based coating is due to its high abrasive and corrosion resistance.

Thus, the process of gas-flame surfacing implying the application of a nickel-based wear-resistant powder on the working surfaces of a friction pair made from low-carbon steel of elevated plasticity must be studied in detail. This is especially important for improving the abrasion resistance of the conical slide frames of the original design, which are part of the mortar mixer.

---

### 3. The aim and objectives of the study

---

The aim of this study is to reduce the magnitude of abrasive wear of the wrist pin and insert in a conical slide frame, which works as part of the screw working body of a mortar mixer and interacts with a soluble mixture used for construction.

To accomplish the aim, the following tasks have been set:

- to construct a mathematical model that would adequately characterize the technological process of gas-flame surfacing by applying a hard alloyed nickel-based wear-resistant powder;
- to simulate at an experimental bench the wear process of a friction pair in the abrasive environment under the applied loads;
- to propose a procedure for determining the magnitude of an axial load experienced by a slide frame during operation;
- to carry out a series of experimental studies to determine the wear of friction pairs in a slide frame with respect to the structural execution of the wrist pin and insert in a slide frame, the articles' materials, and a working environment;
- to determine the optimum parameters for the technological process of gas-flame surfacing of the working surfaces of the insert and wrist pin in a slide frame of the mortar mixer.

**4. Materials and methods to study the abrasive resistance of a slide frame in a mortar mixer**

A material chosen for the manufacture of the insert and wrist pin with the aim of applying a wear-resistant coating was steel 25. This is a low carbon structural steel of small strength but high plasticity, used for the manufacture of various components from rolled steel, forgings, pipes, sheets, strips and wire. The finishing heat treatment is not required for the case under consideration.

The chemical composition and mechanical properties of steel 25 are given in Table 1.

At the beginning of machining, the working surfaces of a friction pair had a roughness of 12.5 μm on the *R<sub>a</sub>* scale. A special burner containing a dispenser for a powdered material was applied at gas-flame surfacing. We used a hard alloyed powder, grade PG10N-0. Its chemical composition is given in Table 2.

The process of surfacing involved a combustible gas, namely the [C<sub>2</sub>H<sub>2</sub>+O<sub>2</sub>] mixture, which could provide for the required melting temperature of a hard alloyed powder. The workpiece was pre-heated to (300...400 °C). The surfacing is followed by a turning treatment using a composite material. The thickness of the newly-formed coating, measured by an ultrasonic flaw detector, is 1 mm. The microstructure of the coating is shown in Fig. 4.

The quality of the newly-formed coating was tested through the adhesion strength ( $\sigma_{ad}^*$ , MPa) between the latter and the base. To this end, a pin detachment method was used and a tensile testing machine.

Adhesion strength between the newly-formed coating and the base material (steel 25) depends on the technological parameters of the surfacing process, namely: C<sub>2</sub>H<sub>2</sub> pressure, consumption of O<sub>2</sub> and the hard alloyed powder. These technological parameters were chosen as the variance factors for the newly created model in order to derive their optimum values. The latter should ensure the maximum adhesion between a wear-resistant coating and the base because its insufficient value could lead to peeling and, consequently, to the loss of abrasive stability (Table 3).

Underlying a mathematical model (the dependence of adhesion strength between a coating and the base on three technological factors) is the equation in the following form:

$$y = b_0 + b_1 \cdot x_1 + b_2 \cdot x_2 + b_3 \cdot x_3 + b_{11} \cdot x_1^2 + b_{22} \cdot x_2^2 + b_{33} \cdot x_3^2 + b_{12} \cdot x_1 \cdot x_2 + b_{13} \cdot x_1 \cdot x_3 + b_{23} \cdot x_2 \cdot x_3. \quad (1)$$

To investigate the wear process in a slide frame after surfacing, we proposed the design of experimental bench (Fig. 5), which simulates the operational process.

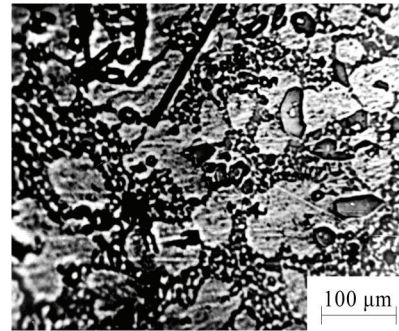


Fig. 4. The coating's microstructure

Table 3

Factor levels and their variance intervals

| Factor levels     | Designations | <i>P</i> <sub>C<sub>2</sub>H<sub>2</sub></sub> , MPa | <i>q</i> <sub>O<sub>2</sub></sub> , l/min | <i>q</i> <sub>PG</sub> , g/min |
|-------------------|--------------|--|---|--------------------------------|
|                   |              | <i>X</i> <sub>1</sub>                                | <i>X</i> <sub>2</sub>                     | <i>X</i> <sub>3</sub>          |
| Upper             | +1           | 0.060  | 7.00                                      | 50.0                           |
| Basic             | 0            | 0.043  | 4.75                                      | 33.5                           |
| Lower             | -1           | 0.026  | 2.50                                      | 17.0                           |
| Variance interval | $\Delta x_i$ | 0.017  | 2.25                                      | 16.5                           |

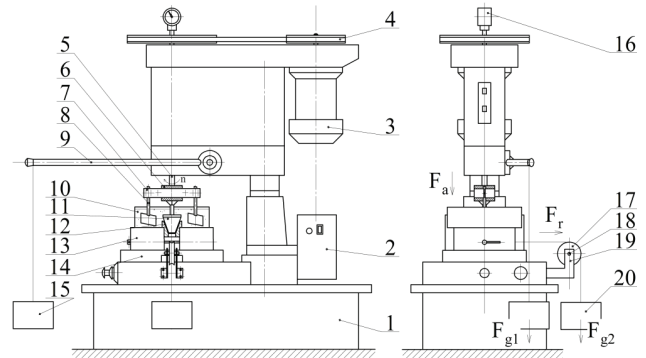


Fig. 5. Structural diagram of the experimental bench

Table 1

Chemical composition and mechanical properties of steel 25 (GOST 1050-2013)

| Material type | Chemical composition, % |           |           |         |          |          |         |         | Mechanical properties, % |                     |                |            |
|---------------|-------------------------|-----------|-----------|---------|----------|----------|---------|---------|--------------------------|---------------------|----------------|------------|
|               | C                       | Si        | Mn        | Ni      | S        | P        | Cr      | Cu      | $\sigma_{ys}$ , MPa      | $\sigma_{ts}$ , MPa | $\Delta_5$ , % | $\psi$ , % |
| Steel 25      | 0.22–0.30               | 0.17–0.37 | 0.50–0.80 | to 0.30 | to 0.035 | to 0.030 | to 0.25 | to 0.30 | 275                      | 450                 | 23             | 50         |

Table 2

Chemical composition of the hard alloyed powder PG10N-01 (TU U 322-19-004-96)

| Base | Cr    | B       | Si      | Fe      | C       | Coating hardness, HRC | Grain size, μm |
|------|-------|---------|---------|---------|---------|-----------------------|----------------|
| Ni   | 14–20 | 2.8–4.2 | 4.0–4.5 | 3.0–7.0 | 0.6–1.0 | 40–62                 | 40–80          |

The principle of the experimental bench operation (Fig. 5), placed atop fixed metal bed 1, is as follows. It is connected to the network of a three-phase current through frequency converter 2 (to control the engine rotation frequency). From electric motor 3 ( $P=0.4\text{ kW}$ ,  $n=1,320\text{ rpm}$ ), via belt drive 4, the rotation is transmitted to spindle 5, which hosts cartridge 6. The cartridge, via clamp 7, is connected to two blades 8, executing a rotational motion clockwise. The examined friction pair is composed of insert 12 and wrist pin 10. Insert 12 is located in the hole at the bottom of tub 10 and is clamped by grip 13. The latter resides on table 14 with a T-groove. Wrist pin 11 is fixed in chuck 6. Tub 10 is filled with a mortar, electric motor 3 is enabled, lever 9 hosts load  $F_{g1}$  15 (simulating the axial load  $F_a$ ), the insert holds load  $F_{g2}$  20 (simulating the radial load  $F_r$ ) using roller 17, axis 18, rack 19. Wrist pin 11, at rotation, is delivered to insert 12. Blades 8 mix a mortar in tub 10, thus providing for the uniformity of the soluble mixture, as well as its feed to the contact area between wrist pin 11 and insert 12. Tachometer 16 controlled the spindle rotation frequency of the experimental bench. The overall view of the experimental bench is shown in Fig. 6.

The preset value for the rotation frequency at which a conical frame operates was 40 rpm. This frequency corresponds to the working value of the mixer shaft speed where the examined slide frames are located.

To determine the magnitude of an axial effort (applied when loading at the experimental bench shown in Fig. 6), we have designed a special single-piston hydraulic device, whose structural diagram and the physical appearance are shown in Fig. 7, 8, respectively.



Fig. 6. Image of the experimental bench

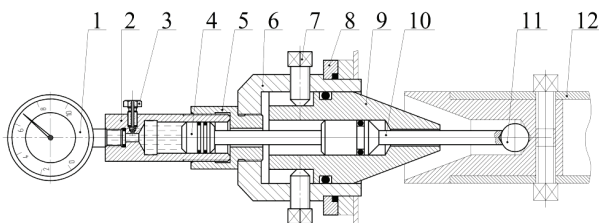


Fig. 7. Structural diagram of the device for determining the axial load: 1 – pressure gauge; 2 – sleeve; 3 – fitting; 4 – piston; 5 – screw sleeve; 6 – body; 7 – adjusting screws; 8 – flange; 9 – wrist pin; 10 – plunger; 11 – ball; 12 – screw shaft

The principle of the device operation is as follows (Fig. 7). During operation, as a result of the axial load, the mixer

shaft moves in the axial direction (from right to left). Ball 11 starts to interact with plunger 10, connected to piston 4. The latter acts on the working fluid that fills the inner cavity of sleeve 2. Pressure gauge 1 registers the generated pressure, as shown in Fig. 9.



Fig. 8. Image of the device for determining the axial load



Fig. 9. Determining the axial load on a frame by the device

The magnitude of axial load  $F_a$ , N, was calculated from formula

$$F_a = p_m \cdot S, \tag{2}$$

where  $p_m$  is the pressure value, registered by a manometer, Pa;  $S$  is the piston's surface area,  $\text{m}^2$ .

When increasing the mobility of a soluble mixture used for construction (defined by DSTU B V.2.7-239:2010) two-fold, the magnitude of the axial load on a slide frame is reduced by 2.5–3 times [4]. The maximum possible axial load on a slide frame (186 N) under a non-stationary mixing mode was registered for the following composition of a cement-sand mortar: 1:5; mobility, 6 cm; the rotation frequency of a working shaft, 40 rpm; with the mortar mixer filled to capacity. This value was used as an axial load during wear tests.

The amount of wear  $I$ , g, was determined based on a change in the mass before and after tests at a non-lever electronic scale (accuracy of measurement, 0.001 g).

The examined samples of the wrist pin and insert were made from the hardened steels of grades 45 (HRC 45...50), KhVG (HRC 60...63), ShKh15 (HRC 62...65), as well as obtained from surfacing (HRC 60...65). The hardness of the samples was determined using a hardness tester under laboratory conditions. Steel 45 was used to manufacture the samples with different values for the angle at the apex of the cone (Fig. 10).

The ultimate result from each series of experiments was the arithmetic mean of the test results from five friction pairs at the experimental bench.



Fig. 10. Examined samples of the wrist pin in a slide frame at angle  $\alpha$  at the apex: 30°, 35°, 40°, 45°, 50° (from left to right)

**5. Results of studying the improved abrasive resistance of a slide frame in a mortar mixer**

To construct a mathematical model and estimate the strength of adhesion between a layer of the surfaced wear-resistant coating of a hard alloyed powder ( $\sigma_{ad}^{\tau}$ , MPa) and the steel base of the frame, we conducted a multifactorial experiment to measure the magnitude of a detachment force by a pin method (see above). Table 4 gives a planning matrix of the multifactorial experiment.

Table 4

Planning matrix of the three-factorial experiment

| No. | $x_1$ | $x_2$ | $x_3$ | $x_1^2$ | $x_2^2$ | $x_3^2$ | $x_1x_2$ | $x_1x_3$ | $x_2x_3$ |
|-----|-------|-------|-------|---------|---------|---------|----------|----------|----------|
| 1   | 1     | 1     | 1     | 1       | 1       | 1       | 1        | 1        | 1        |
| 2   | -1    | 1     | 1     | 1       | 1       | 1       | -1       | -1       | 1        |
| 3   | 1     | -1    | 1     | 1       | 1       | 1       | -1       | 1        | -1       |
| 4   | -1    | -1    | 1     | 1       | 1       | 1       | 1        | -1       | -1       |
| 5   | 1     | 1     | -1    | 1       | 1       | 1       | 1        | -1       | -1       |
| 6   | -1    | 1     | -1    | 1       | 1       | 1       | -1       | 1        | -1       |
| 7   | 1     | -1    | -1    | 1       | 1       | 1       | -1       | -1       | 1        |
| 8   | -1    | -1    | -1    | 1       | 1       | 1       | 1        | 1        | 1        |
| 9   | 1     | 0     | 0     | 1       | 0       | 0       | 0        | 0        | 0        |
| 10  | -1    | 0     | 0     | 1       | 0       | 0       | 0        | 0        | 0        |
| 11  | 0     | 1     | 0     | 0       | 1       | 0       | 0        | 0        | 0        |
| 12  | 0     | -1    | 0     | 0       | 1       | 0       | 0        | 0        | 0        |
| 13  | 0     | 0     | 1     | 0       | 0       | 1       | 0        | 0        | 0        |
| 14  | 0     | 0     | -1    | 0       | 0       | 1       | 0        | 0        | 0        |
| 15  | 0     | 0     | 0     | 0       | 0       | 0       | 0        | 0        | 0        |
| 16  | 0     | 0     | 0     | 0       | 0       | 0       | 0        | 0        | 0        |
| 17  | 0     | 0     | 0     | 0       | 0       | 0       | 0        | 0        | 0        |

In the course of our study, we determined a confidence interval for each experiment and compared it with the total spread of values.

We have derived the coefficients for a regression equation, whose significance was checked by comparing the estimated value of the Student criterion with a tabular value; the results are given in Table 5.

Table 5

Regression equation coefficients

| $b_0$    | $b_1$    | $b_2$    | $b_3$    | $b_{11}$ |
|----------|----------|----------|----------|----------|
| 44.697   | 0.226    | 0.119    | 0        | -0.657   |
| $b_{22}$ | $b_{33}$ | $b_{12}$ | $b_{13}$ | $b_{23}$ |
| 0.029    | -0.436   | -0.079   | -0.041   | -0.328   |

By fitting the regression coefficients into the equation of a mathematical model (1), we obtain:

$$y = 44.697 + 0.226 \cdot x_1 + 0.119 \cdot x_2 - 0.657 \cdot x_1^2 + 0.029 \cdot x_2^2 - 0.436 \cdot x_3^2 - 0.079 \cdot x_1 \cdot x_2 - 0.041 \cdot x_1 \cdot x_3 - 0.328 \cdot x_2 \cdot x_3. \quad (3)$$

After moving from the encoded values to actual ones, by fitting the derived ones into formula (3), we obtain:

$$y = 35.964 + 223.51 \cdot P_{C_2H_2} + 0.383 \cdot q_{O_2} + 0.156 \cdot q_{PG} - 2273.356 \cdot P_{C_2H_2}^2 + 0.006 \cdot q_{O_2}^2 - 0.002 \cdot q_{PG}^2 - 2.065 \cdot P_{C_2H_2} \cdot q_{O_2} - 0.146 \cdot P_{C_2H_2} \cdot q_{PG} - 0.009 \cdot q_{O_2} \cdot q_{PG}. \quad (4)$$

The resulting assessment of suitability of the mathematical model in the form of a functional dependence (4) was carried out based on a Fisher criterion. The calculations demonstrated that the model is adequate. The mean value of a relative error between the calculated and experimental values does not exceed 2.8 %.

Fig. 11 shows the obtained three-dimensional graphic dependences of the adhesion strength of the wear-resistant coating made from the surfaced solid alloy PG10N-01 on: oxygen and powder consumption (Fig. 11, a); acetylene pressure and the powder consumption (Fig. 11, b); acetylene pressure and oxygen consumption (Fig. 11, c).

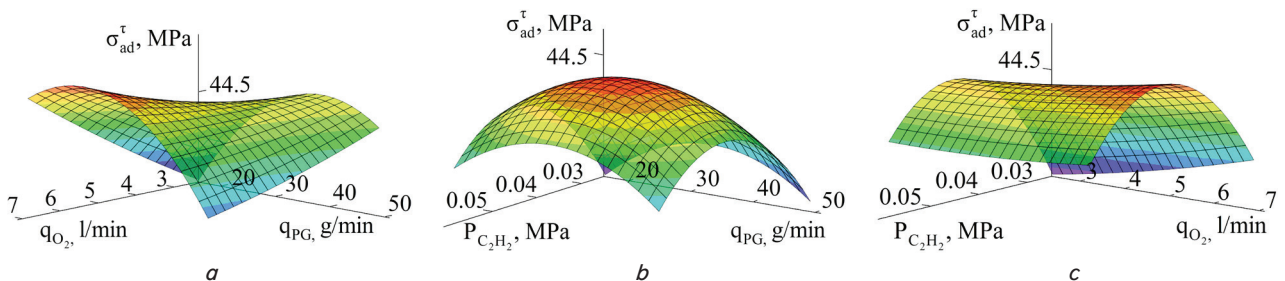


Fig. 11. Three-dimensional graphic dependences of strength: a -  $\sigma_{ad}^{\tau} = f(q_{O_2}; q_{PG})$ ,  $P_{C_2H_2} = 0.043$  MPa,  $q_{O_2} = 2.5 \dots 7$  l/min,  $q_{PG} = 17 \dots 50$  g/min; b -  $\sigma_{ad}^{\tau} = f(P_{C_2H_2}; q_{PG})$ ,  $P_{C_2H_2} = 0.026 \dots 0.060$  MPa;  $q_{O_2} = 4.75$  l/min;  $q_{PG} = 17 \dots 50$  g/min; c -  $\sigma_{ad}^{\tau} = f(P_{C_2H_2}; q_{O_2})$ ,  $P_{C_2H_2} = 0.026 \dots 0.060$  MPa,  $q_{O_2} = 2.5 \dots 7$  l/min,  $q_{PG} = 33.5$  g/min

Our tests at the experimental bench (Fig. 12) established that the interacting surfaces of the wrist pin and insert in a slide frame that operate in an abrasive environment (a soluble mixture used for construction) have lines. They are the characteristic elements of abrasive wear. In addition, there are signs of corrosion. Consequently, the abrasive-corrosion wear occurs, which could be minimized by surfacing a hard alloyed nickel-based coating with not only a high abrasive resistance but the corrosion resistance as well.



Fig. 12. Signs of abrasive-corrosion wear in the components from a friction pair in the slide frame of a mortar mixer: *a* – insert; *b* – wrist pin

Fig. 13 shows the results from our experimental study in the form of charts illustrating the dependences of a friction pair’s wear on time and structural execution.

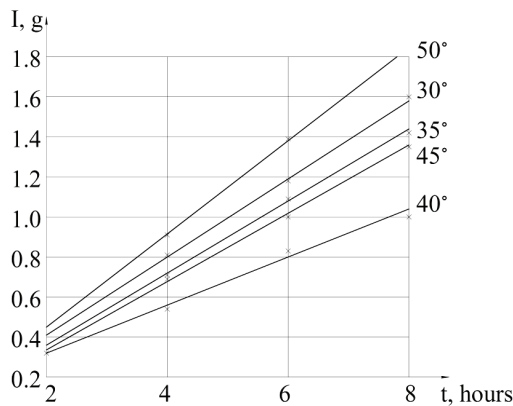


Fig. 13. Dependence of wear amount in the wrist pin *I*, g, over time *t*, hours (the total load on a frame  $F_{\Sigma}=375$  N; the samples’ material – steel 45; a cement-sand mortar, 1:5; mobility, 6 cm; 30°, 35°, 40°, 45°, 50° – angle at the apex of the cone)

Fig. 14 shows the results from a series of our experimental studies aimed at determining a wear amount of the friction pairs made from different materials (45, KhVG, ShKh15) that interact with a soluble mixture used for construction, with an angle at the apex of the cone of 40°.

Following the application on the steel base of the wrist pin in a frame at an angle at the apex of 40° of the hard alloyed coating on the friction surface at the optimum parameters of surfacing ( $q_{PG}=33.5$  g/min,  $q_{O_2}=7.0$  l/min,  $P_{C_2H_2}=0.043$  MPa), we again estimated the wear amount in a fashion similar to the conducted experiment involving steel samples (Fig. 15).

A maximum of the adhesion strength, based on the examination of function (4) for extrema, corresponds to the following technological parameters:  $q_{O_2}=7.0$  l/min,  $q_{PG}=$

$= 27.29$  g/min (Fig. 11, *a*);  $P_{C_2H_2}=0.046$  MPa,  $q_{PG} = 33.37$  g/min (Fig. 11, *b*);  $P_{C_2H_2}=0.043$  MPa,  $q_{O_2} = 7.0$  l/min (Fig. 11, *c*).

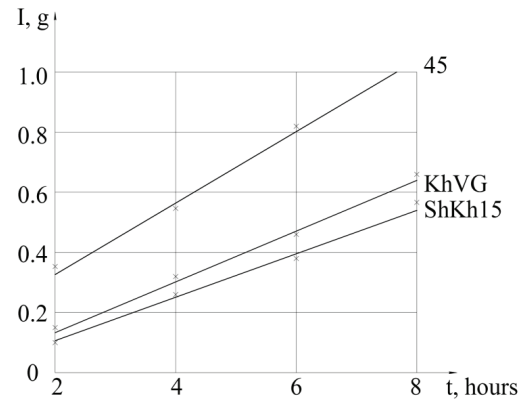


Fig. 14. Dependence of wear amount in the wrist pin, *I*, g, a material, over time *t*, hours (the total load on a frame  $F_{\Sigma}=375$  N; the samples’ material – steel 45, KhVG, ShKh15; a cement-sand mortar, 1:5; mobility, 6 cm; angle at the apex, 40°)

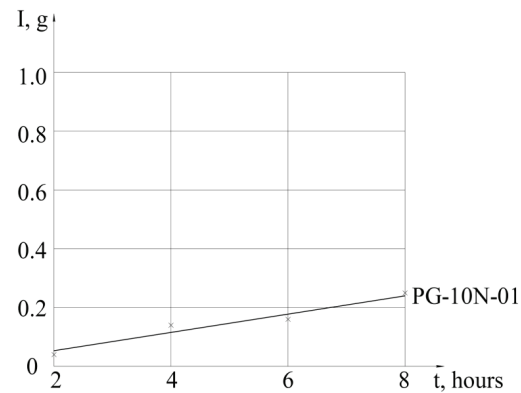


Fig. 15. Dependence of wear amount in the wrist pin, *I*, g, over time *t*, hours (the total load on a frame  $F_{\Sigma}=375$  N; the friction surfaces’ material, PG-10N-01; a cement-sand mortar, 1:5, mobility, 6 cm; angle at the apex, 40°)

The use of a wear-resistant hard alloyed coating, applied by a method of gas-flame surfacing, is an effective technique for a significant reduction in the magnitude of abrasive wear of the wrist pin and insert in a conical frame.

## 6. Discussion of results of forming the shape of external profile surfaces

The results of the current study include an increase in the abrasive resistance of the rubbing parts in the slide frame of a mortar mixer, which is confirmed by Fig. 11–13. This is achieved through the use of gas-flame surfacing by applying a wear-resistant hard alloyed nickel-based powder, the grade PG-10N-01. The result is the formed coating with a complex structure, in which the layers of particles from the surfaced high-hardness material alternate with the oxide layers. Such a character of the structure is the reason for the high wear resistance of the surfaced layer. The powder is applied onto the working surfaces of the wrist pin and insert made from steel 25 with high plasticity and low cost.

However, the findings from our scientific study are valid for a particular friction pair, specifically the insert and wrist pin in a slide frame, because it has some design features.

When examining a mathematical model for determining the optimal parameters of applying a hard alloyed coating by a method of gas-flame surfacing, we built the three-dimensional charts to investigate the strength of adhesion between a coating and the base at paired interactions between the study factors (Fig. 11). Varying the factors of oxygen and powder consumption has revealed that the adhesion strength increases at the upper value of oxygen consumption and the medium value of powder consumption within the predefined range (Fig. 11, *a*). When varying the factors of acetylene pressure and powder consumption, it has been found that the adhesion strength increases when choosing the medium values of acetylene pressure and powder consumption within the predefined limits (Fig. 11, *b*). Varying the factors of acetylene pressure and oxygen consumption has established that the adhesion strength increases at the medium acetylene pressure and the upper value of oxygen consumption within the specified limits (Fig. 11, *b*). By combining the variance in all three charts at the same time, we have found that the optimal parameters for applying a coating would be: the medium value of powder consumption, the upper value of oxygen consumption, and the medium value of acetylene pressure, that is  $q_{PG}=33.5$  g/min,  $q_{O_2}=7.0$  l/min,  $P_{C_2H_2}=0.043$  MPa. This is explained by the maximum value of adhesion strength between the applied wear-resistant coating and the base of 45 MPa, which is determined using a pin detachment method by applying a tensile testing machine.

Fig. 13 shows that the angle at the apex of the cone, which is equal to  $40^\circ$ , ensures the optimum ratio between the axial and radial loads on a frame during the operation of a screw mixer. This, in turn, leads to a decrease in the amount of wear. The increase or decrease in this angle relative to the optimal value could lead to a negative impact: in the first case – the radial load, and in the second case – the axial load. That would affect the increase in the amount of wear.

The indicators obtained for the ball bearing steel of grade ShKh15 and the instrumental steel of grade KhVG are satisfactory compared to steel 45, so it is not recommended to use the latter for the manufacture of bearings (Fig. 14). At the slide speed of 7.54 m/min., the average wear intensity of a wrist pin was 0.080 g/hour – for steel KhVG, ShKh15; 0.130 g/hour – for steel 45.

As regards the impact exerted on the wear amount in a slide frame by the type of a mortar used for construction and its mobility, one should note the following. Earlier studies [4] found that increasing the mobility of a mortar and transferring from the cement-sand and complex mortars to lime-sand decrease the quantity of power consumed by a drive. That would result, in this case, to a decrease in the magnitude of the torque and the total load. Thus, the wear of a slide frame would decrease while its durability could increase.

At the speed of sliding of 7.54 m/min. (Fig. 15), the average wear intensity of a wrist pin was 0.032 g/hour for the hard alloyed coating PG-10N-01, which is about 2.5 times better than that for KhVG or ShKh15.

It should be noted that our study was performed for the components of a bearing frame in a mortar mixer (the insert and wrist pin) made from steel 25, followed by the gas-flame surfacing of a hard alloyed nickel-based powder, the grade PG10N-01. The frame is used in the body of a reversible screw mixer, rotating at a constant frequency of 40 r/min. During operation, the insert and wrist pin are in contact with each other and a working environment, which is a soluble mixture used for construction.

A promising direction to improve the wear resistance of a slide frame is not to use the technology of gas-flame surfacing, but melting [1]. The essence of the latter is not surfacing, but melting, with a burner, the wear-resistant material already applied onto the surface of rubbing parts in the wrist pin and insertion in a frame. That could make it possible to avoid splashing a molten powder, which is characteristic of surfacing, and to simplify the design of a burner. However, the proposed technology must be studied in detail, in order to address the adhesion strength between a material, already fused, and the base, as well as to search for the optimal modes in the technological process.

---

## 7. Conclusions

---

1. We have constructed a mathematical model in the form of a functional dependence that adequately describes the technological process of gas-flame surfacing. At the paired interaction of factors, we have built the three-dimensional graphic dependences of the adhesion strength for a wear-resistant coating of the wrist pin and insert in a slide frame on the technological parameters.

2. Using an experimental bench based on a desktop vertically-drilling machine, we have simulated the process of wearing a slide frame in an abrasive environment under the action of applied loads. There were characteristic signs of the abrasive-corrosion wear of the wrist pin and insert in a frame.

3. A procedure has been proposed to determine the amount of the axial load perceived by a frame. It is 186 N.

4. A series of experimental studies has shown that the best option for a structural execution of the wrist pin and insert is the angle at the apex of  $40^\circ$ . Forming a wear-resistant coating based on the hard alloyed powder PG-10N-01 ensures excellent durability indicators. They exceed those for steel ShKh15 by about 2.5 times.

5. We have defined the optimum parameters for the technological process of gas-flame surfacing, which provide for a maximum value of the adhesion strength between a newly-formed wear-resistant coating and the base, 45 MPa, namely: powder consumption, 33.5 g/min; oxygen consumption, 7.0 l/min; acetylene pressure, 0.043 MPa.

---

## References

1. Biletskyi, V. S. (Ed.) (2004). *Mala hirnycha entsyklopediya*. Donetsk: Skhidnyi vydavnychiy dim, 640.
2. Onyshchenko, O. H., Popov, S. V. (2005). Rehulovani konichni pidshypnyky kovzannia mobilnoi rozchynozmishuvalnoi ustanovky URZ-3,8. *Eastern-European Journal of Enterprise Technologies*, 6 (1 (18)), 45–47.
3. Onyshchenko, O. H., Vashchenko, K. M., Popov, S. V. (2007). *Perspektyvy vykorystannia rozchynozmishuvalnoi ustanovky URZ-3,8 na budivelnykh maidanchykakh Ukrainy. Sovremennye problemy stroitel'stva*. Donetsk: Donetskii PromstroyNIIproekt, 138–144.

4. Kravchenko, S., Popov, S., Gnitko, S. (2016). The working pressure research of piston pump RN-3.8. *Eastern-European Journal of Enterprise Technologies*, 5 (1 (83)), 15–20. doi: <https://doi.org/10.15587/1729-4061.2016.80626>
5. Popov, S., Vasilyev, A., Lednik, R. (2015). Theoretical wear research of conical friction bearing. *Technology Audit and Production Reserves*, 2 (1 (22)), 60–64. doi: <https://doi.org/10.15587/2312-8372.2015.41395>
6. Kaplun, P., Gonchar, V., Bodnar, R. (2013). Enhancement of steel wear resistance in corrosive and abrasive medium. *Interdisciplinary integration of science in technology, education and economy. Bydgoszcz-Poland*, 320–329.
7. Sobolev, V. V., Guilemany, J. M., Miguel, J. R., Calero, J. A. (1996). Influence of in-flight dissolution process on composite powder particle (WC-Ni) behaviour during high velocity oxy-fuel spraying. *Surface and Coatings Technology*, 81 (2-3), 136–145. doi: [https://doi.org/10.1016/0257-8972\(95\)02481-6](https://doi.org/10.1016/0257-8972(95)02481-6)
8. Sobolev, V. V., Guilemany, J. M., Miguel, J. R., Calero, J. A. (1996). Influence of thermal processes on coating formation during high velocity oxy-fuel (HVOF) spraying of WC-Ni powder particles. *Surface and Coatings Technology*, 82 (1-2), 121–129. doi: [https://doi.org/10.1016/0257-8972\(95\)02657-6](https://doi.org/10.1016/0257-8972(95)02657-6)
9. Shrestha, S., Hodgkiess, T., Neville, A. (2005). Erosion-corrosion behaviour of high-velocity oxy-fuel Ni-Cr-Mo-Si-B coatings under high-velocity seawater jet impingement. *Wear*, 259 (1-6), 208–218. doi: <https://doi.org/10.1016/j.wear.2005.01.038>
10. Dent, A. H., Horlock, A. J., McCartney, D. G., Harris, S. J. (2001). Microstructural characterisation of a Ni-Cr-B-C based alloy coating produced by high velocity oxy-fuel thermal spraying. *Surface and Coatings Technology*, 139 (2-3), 244–250. doi: [https://doi.org/10.1016/s0257-8972\(01\)00996-3](https://doi.org/10.1016/s0257-8972(01)00996-3)
11. Sang, K., Li, Y. (1995). Cavitation erosion of flame spray weld coating of nickel-base alloy powder. *Wear*, 189 (1-2), 20–24. doi: [https://doi.org/10.1016/0043-1648\(95\)06608-x](https://doi.org/10.1016/0043-1648(95)06608-x)
12. Huang, F., Xu, H., Liu, W., Zheng, S. (2018). Microscopic characteristics and properties of titaniferous compound reinforced nickel-based wear-resisting layer via in situ precipitation of plasma spray welding. *Ceramics International*, 44 (6), 7088–7097. doi: <https://doi.org/10.1016/j.ceramint.2018.01.148>
13. Janka, L., Berger, L.-M., Norpoth, J., Trache, R., Thiele, S., Tomastik, C. et. al. (2018). Improving the high temperature abrasion resistance of thermally sprayed Cr<sub>3</sub>C<sub>2</sub>-NiCr coatings by WC addition. *Surface and Coatings Technology*, 337, 296–305. doi: <https://doi.org/10.1016/j.surfcoat.2018.01.035>
14. Kazasidis, M., Yin, S., Cassidy, J., Volkov-Husović, T., Vlahović, M., Martinović, S. et. al. (2020). Microstructure and cavitation erosion performance of nickel-Inconel 718 composite coatings produced with cold spray. *Surface and Coatings Technology*, 382, 125195. doi: <https://doi.org/10.1016/j.surfcoat.2019.125195>